EGYPTIAN DENTAL JOURNAL
www.eda-egypt.org
VOL. 69, 1161:1180, APRIL, 2023
PRINT ISSN 0070-9484 • ONLINE ISSN 2090-2360
ORAL MEDICINE, X-RAY, ORAL BIOLOGY AND ORAL PATHOLOGY
Submit Date : 21-02-2023 • Accept Date : 21-03-2023 • Available online: 01-04-2023 • DOI : 10.21608/edj.2023.195400.2458

A COMPARATIVE HISTOLOGICAL AND IMMUNOHISTOCHEMICAL STUDY ON THE EFFECT OF MORINGA OIL AND SESAME OIL ON THE SUBMANDIBULAR GLANDS OF CISPLATIN TREATED ALBINO RATS

Hend El-Messiry*, Dina Fouad El Shaer ** *and* Iman Ahmed Fathy*

ABSTRACT

Cisplatin, also known as CP, is an antineoplastic drug that is utilised most frequently in the chemotherapeutic treatment of a wide variety of cancers. Because of the high levels of monounsaturated fatty acids, sterols, tocopherols, and proteins that are rich in sulfated amino acids that are found in Moringa oleifera oil (MO) and Sesame oil (SO) seeds, these two plant species have the potential to become valuable resources. A comparison of the protective effects of MO and SO against the damage caused by CP in the submandibular glands of albino rats was the purpose of this study. 45 rats were randomly assigned to one of four groups: group I served as the control, group II received a single intraperitoneal injection of CP (5 mg/kg), group III received MO (5mg/kg/day) orally, and group IV received SO (5mg/kg/day) orally. Histopathological changes such as cytoplasmic vacuolation, irregular dark shrunken nuclei, loss of normal acinar architecture, irregular and distorted ducts with focal loss of their lining epithelium and basement membrane, and congested blood vessels were observed in the CP group. These changes were observed in the pancreatic polyps. In the CP group, we saw large increases in the expression of -SMA and Caspase-3, and significant decreases in the expression of PCNA and PAS. These findings showed some sign of improvement in the groups that had been treated with MO and SO. According to the findings of this investigation, both MO and SO were able to mitigate the harm produced by cisplatin, with MO showing a very tiny advantage over SO.

KEYWORDS: Cisplatin, Moringa, Sesame, immunohistochemical, submandibular gland

* Oral Biology Department, Faculty of Dentistry Ain Shams University Cairo Egypt
** Histology and Cell Biology Department, Faculty of Medicine, Tanta University, Tanta, Egypt.

INTRODUCTION

Chemotherapy is most used as the primary treatment modality for a select number of different types of cancer, as palliative treatment for specific types of advanced tumours, and as an adjuvant treatment before, during, or after local treatment (surgery and/or radiotherapy). The elimination of metastases and an improvement in the management of local tumours are the goals of chemotherapy (Dasari and Tchounwou, 2014; Ojima et al., 2018). Yet, chemotherapy can also have a cytotoxic effect on healthy cells and tissues in addition to the cells it targets in cancerous ones. The type of therapy, the amount of treatment, and how long it is administered all affect its cytotoxic effect (Abdulmonem, 2020).

Cisplatin is a powerful chemotherapeutic medicine that is used quite frequently. This is because of the therapeutic properties that it possesses. Despite this, cisplatin has been linked to several adverse effects, including neurotoxicity, ototoxicity, and renal toxicity. Because it causes oral issues such as mucositis (stomatitis), xerostomia (dry mouth), a tendency to bleed, dental caries, and loss of taste, which can lead to an increase in oral infections, it also affects the submandibular and parotid salivary glands. This is because it produces oral issues such as mucositis (stomatitis). It is possible that the generation of reactive oxygen species (ROS) and lipid peroxidation, both of which lead to oxidative tissue damage, are responsible for its cytotoxicity (Hany et al., 2017; Tchounwou et al., 2021).

Moringa oleifera (MO) is a tree in the family of Moringaceae that grows abundantly in many tropical and subtropical countries. It has numerous health and environmental benefits. Each part of this plant (roots, seeds, seed oil, leaves, fruit, and flowers) has an important and distinct function (Abdel-Latif et al., 2022). Moringa oleifera seed oil includes several fatty acids (monounsaturated fatty acids, polyunsaturated fatty acids, oleic acid, palmitic acid, behenic acid, and linolenic acid), in addition to calcium and - tocopherols. It is hence anticancer, antioxidant, hepatoprotective, and insecticidal. Moreover, cosmetic, pharmaceutical and medical companies use moringa oleifera seed oil (Fu et al., 2021).

Sesame (Sesamum indicum Linn.) is a member of the Pedaliaceae family and is extensively used in oriental cuisine. In addition, multiple lines of evidence from both traditional and contemporary medicine indicate the medicinal properties of sesame. This plant contains significant amounts of many phytochemicals, such as phenolic acids and lignan oils. These phytochemicals have demonstrated potential as natural antioxidants for food preservation and medical applications (Mili et al., 2021; Guo et al., 2022).

Sesame seed contains moisture, crude oil, crude proteins, carbs, crude fibre, and ash. Sesame oil (50% of total seed content) is an excellent source of monounsaturated and polyunsaturated fatty acids. According to previous research, the antioxidant capabilities of sesame seed may be attributable to sesamol, sesamolin, pinoresinol, and sesaminol, as well as vitamin E. (Kheirati Rounizi et al., 2021). Sesame oil possesses anti-inflammatory, antiapoptotic, antihypertensive, antioxidant, and hypocholesterolemic properties (Fan et al., 2017a&b; Beloucif et al., 2021).

The salivary glands are essential for dental and general health. Its parenchyma is continuously exposed to a variety of local and systemic conditions that can modify its usual histological architecture (Ayuob et al., 2019; Abdulmonem, 2020). Consequently, we found it intriguing to assess the possible ameliorative effects of safe doses of moringa and sesame oils on the submandibular salivary gland damage caused by cisplatin in albino rats.

MATERIALS AND METHODS

This study utilized adult male albino rats (n=45) weighing between 200 and 250 grams. In the animal house of "The Medical Research Center" at Ain-Shams University, rats were housed in separate cages with five rats per cage for the duration of the

experimental period. Rats were maintained under regulated conditions of temperature, humidity, dark-light cycle, ventilation, and a steady diet of fresh vegetables and dried bread. During the duration of the experiment, tap water was available at will. This experiment was conducted under the supervision of a veterinary specialist from the time the animals were housed until the Ain Shams incinerator disposed of the sacrificial bodies. Animal procedures were approved by Research Ethics Committee, Ain Shams University (approval number: FDASU-REC IR022219).

Study design:

1. **Group I (control group):** included 15 rats were subdivided equally into 3 subgroups (5 rats each) as follows:

- Subgroup Ia: 5 rats were left untreated and provided an ordinary diet.
- Subgroup Ib: 5 rats were treated with moringa oil only, daily for 10 days with a dose of 5mg/kg body weight via an oropharyngeal tube (Moawad et al., 2016).
- Subgroup Ic: 5 rats were treated with sesame oil only, daily for 10 days with a dose of 5mg/kg body weight via an oropharyngeal tube (Ali et al., 2020).

2. **Group II (CP group)**: included 10 rats were given a single dose of cisplatin (5 mg/kg body weight) injected via intra-peritoneal injection (**Antunes et al., 2000**).
3. **Group III (MO+CP group):** included 10 rats that were given cisplatin in a similar dose and route of administration as group II, concomitant with moringa oil in a similar dose and route of administration as subgroup Ib.
4. **Group IV (SO+CP group):** included 10 included rats were given cisplatin in the same dose and route of administration of group II, concomitant with sesame oil in the same dose and route of administration of subgroup Ic.

Reagents:

- **Cisplatin** (CAS Number 15663-27-1) was purchased from Sigma-Aldrich (St. Louis, MO).
- **Moringa and sesame oil** were supplied by Prof. Dr Mostafa El-Messiry, a national research institute.

The Moringa oil was extracted from the seeds of Moringa Olifera at a national research facility using the cold pressing process. M. oleifera seeds were dried in sun for 2 to 3 days, then were transferred to a shell removing the unit, to get the kernels. kernels were subsequently dried for a week at room temperature. On the first day, the kernels were weighed and poured into the receiving funnel of the cold presser. The oil was dripped and collected in a container with a known weight. The weight of the oil was determined by subtracting the weight of the oil container. Impurities and protein residues were eliminated using sedimentation. The sedimented oil was decanted and filtered through filter cloth with a pore size of five to six microns on the fourth day (Janaki and Yamuna, 2015).

Sesame oil was supplied as 100% cold-pressed virgin sesame oil. The plant material was purified in a national research institute from broken and damaged seeds, and sedimentation was used to remove solid impurities from fresh cloudy oil extracted by pressing process. Before pressing, the preconditioning of seeds was done at less than 50°C. Cold-pressed (CP) extraction was performed through a Komet single-screw oil presser. To avoid degrading processes, the temperature was maintained at less than 45°C during cold pressing **(Kostadinović Veličkovska et al., 2015).**

Samples preparation:

After the trial, rats were sacrificed by anaesthetic overdose (thiopental sodium, 150mg/kg), and their submandibular salivary glands were promptly dissected (Elgamily and Denewar, 2020). The bodies of the rats were carefully disposed of in the hospital's incinerator. Both sides of the submandibular salivary glands of rats were extracted and

stained with Hematoxylin and Eosin (H&E), PAS, and immunohistochemical stains for Caspase-3, PCNA, and -SMA.

The specimens were dehydrated in increasing alcohol concentrations, cleaned in xylene, impregnated, and embedded in paraffin blocks before being sliced to a thickness of 4-5 microns with a microtome so that they could be mounted on slides. Thereafter, slices were stained with hematoxylin and eosin (H&E) and periodic acid-Schiff (PAS) for routine histological evaluation (Gamble, 2008). Using immunohistochemistry, several specimens were stained to identify PCNA, Caspase-3, and -SMA. fragments of paraffin Homogenized with 3,3′-diaminobenzidine (DAB) hydrogen peroxide, counterstained with Mayer's hematoxylin, dehydrated, cleaned, and mounted with DPX. Negative controls were conducted by removing the primary antibodies and substituting non-immune serum in their place. The Rat spleen, human tonsil, and adult vascular smooth muscle cells served as positive controls for PCNA (Buchwalow and Bocker, 2010).

- **Morphometric study:**

A light microscope (Leica DM500, Switzerland) connected to a digital camera (Leica ICC50, Switzerland) was used to capture the images. The morphometric study was performed using the software of the computerized image analyzer program "ImageJ" (version 1.48v National Institute of Health, Bethesda, Maryland, USA). Five different non-overlapping randomly selected fields from each slide in each group were examined at a magnification of 400 to quantitatively evaluate:

1- The mean acinar diameter (μm) in H&E-stained sections **(Hussein, 2020).**

2- The mean percentage of PCNA positive cells (Proliferation Index) is calculated as the number of positive cells x 100 / total number of cells **(Köroğlu et al., 2019).**

3- The mean area percentage of PAS, caspase-3, and α-SMA **(El Sadik et al., 2018).**

Statistical analysis:

The morphometric analysis yielded mean values plus standard deviation (SD) data. One-way Analysis of Variance (ANOVA) was performed to compare the groups under study. When the ANOVA test produced statistically significant results, Tukey's post hoc test was conducted. A probability value (P-value) of 0.05 was determined to be statistically significant. The statistical analysis was conducted using Statistical Program for the Social Science (SPSS® IBM 25, United States) software (Dawson and Trapp, 2004).

RESULTS

During the trial period, no evidence of sickness or mortality was seen among the rats. In addition, there were no statistically significant changes in the histological and immunohistochemical findings between the subgroups of control group I. (Ia, Ib, Ic). Simplifying the presentation of our results, we designated them as the control group (I) in tables and figures.

Histological Results:

Hematoxylin & Eosin (H&E) staining

-Group I (control group)

Hematoxylin and eosin-stained sections that were obtained from all control subgroups showed the same normal histological and architectural features of the rat's submandibular salivary gland. The gland was divided into lobules separated by thin connective tissue septa extending from the capsule. Each lobule contained closely packed seromucous acini and intralobular ducts (intercalated, striated, and granular convoluted) surrounded by connective tissue stroma. The acini appeared spherical in shape and each acinus was lined with a single layer of pyramidal-shaped cells having rounded basal basophilic nuclei and moderately basophilic cytoplasm. Concerning the duct portion; the intercalated ducts were lined by short cuboidal cells having basophilic cytoplasm and centrally

located rounded nuclei. The striated ducts were lined by columnar cells with central rounded nuclei, eosinophilic cytoplasm, and basal striations. The granular convoluted tubules (GCTs) were lined with high columnar epithelial cells having acidophilic cytoplasm, large rounded basal nuclei, and apical eosinophilic granules. Whereas the excretory ducts were lined by pseudostratified columnar epithelium and were surrounded by fibrous connective tissue stroma that contained blood vessels (Fig.1- A & B).

- Group II (cisplatin group)

The Cisplatin group revealed remarkable structural alterations in the acini and ducts in comparison to those of the control group. Acini and ducts appeared irregular and shrunken, with a space surrounding some shrunken ducts. Some GCTs showed disturbed architecture with clumping of their granular content and disruption of their basal cell membrane (Fig.2-A). Some excretory ducts were dilated and exhibited loss of the pseudo stratification with some nuclei appearing flattened and apically displaced while others appeared karyolitic. In addition, ducts appeared distorted with focal loss of their lining epithelium and basement membrane. Stagnant secretion was observed in the lumen of some ducts (Fig.2-B). Moreover, numerous acini showed irregular or dark shrunken nuclei compressed by variable-sized cytoplasmic vacuoles. Disturbed ducts were noticed with cytoplasmic vacuoles in their ductal cells and loss of the lining epithelium as well as disrupted basal cell membrane (Fig.2-C). Furthermore, there were some areas in the gland that revealed loss of the normal acinar architectural features and some acinar cells showed a signet ring appearance (Fig.2-D). In addition, dilated congested blood vessels were noticed (Fig.2-E).

- Group III (moringa oil + cisplatin group)

Sections of submandibular glands obtained from rats that received moringa oil concomitantly with cisplatin in (group III), revealed mild structural alterations as compared to the cisplatin group. Some areas showed acini with cytoplasmic vacuolation and few destructed ducts as well as mildly congested blood capillaries. Few GCTs showed reduced acidophilic content in a few granular ductal cells and clumping of the granular content in others. (Fig. 3- A & B)

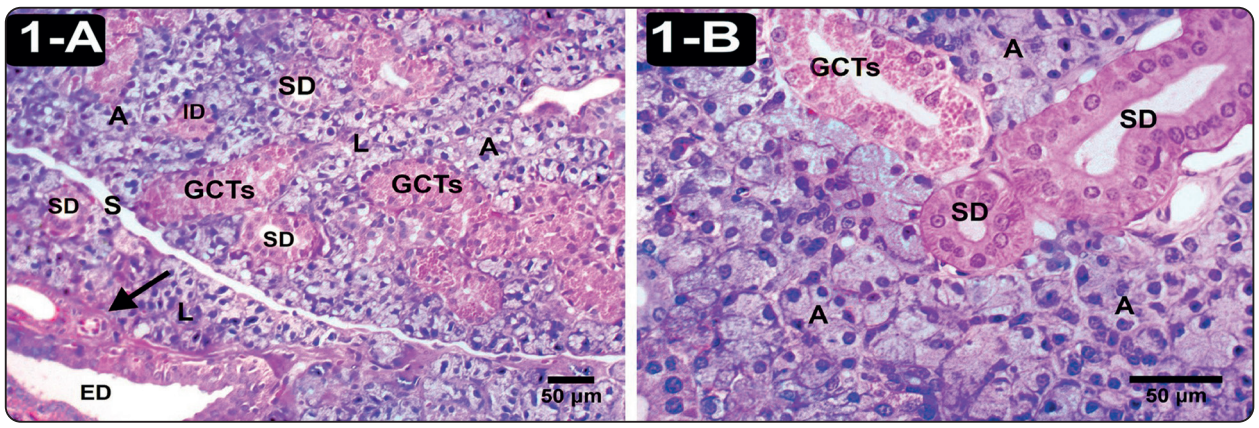

Fig. (1): (A&B) Photomicrographs of submandibular gland sections from group I (control group) showing: (A) Lobules (L) are separated by thin connective tissue septa (S) and each lobule consists of closely packed serous acini (A) which are lined by pyramidal shaped cells having rounded basal basophilic nuclei and basophilic cytoplasm. The intercalated ducts (ID) are lined by simple cuboidal epithelium, the striated ducts (SD) are lined by columnar cells having oval nuclei, and the granular convoluted tubules (GCTs) are lined by columnar cells having acidophilic cytoplasm, large rounded basal nuclei, and apical eosinophilic granules. The excretory ducts (ED) are lined by pseudostratified columnar epithelium and surrounded by variable-sized blood vessels (arrow). (B) Higher magnification of a submandibular gland shows the acini (A), the striated ducts (SD), and the granular convoluted tubules (GCTs). (H&E X 200 A, X 400 B, Bar: 50 μm).

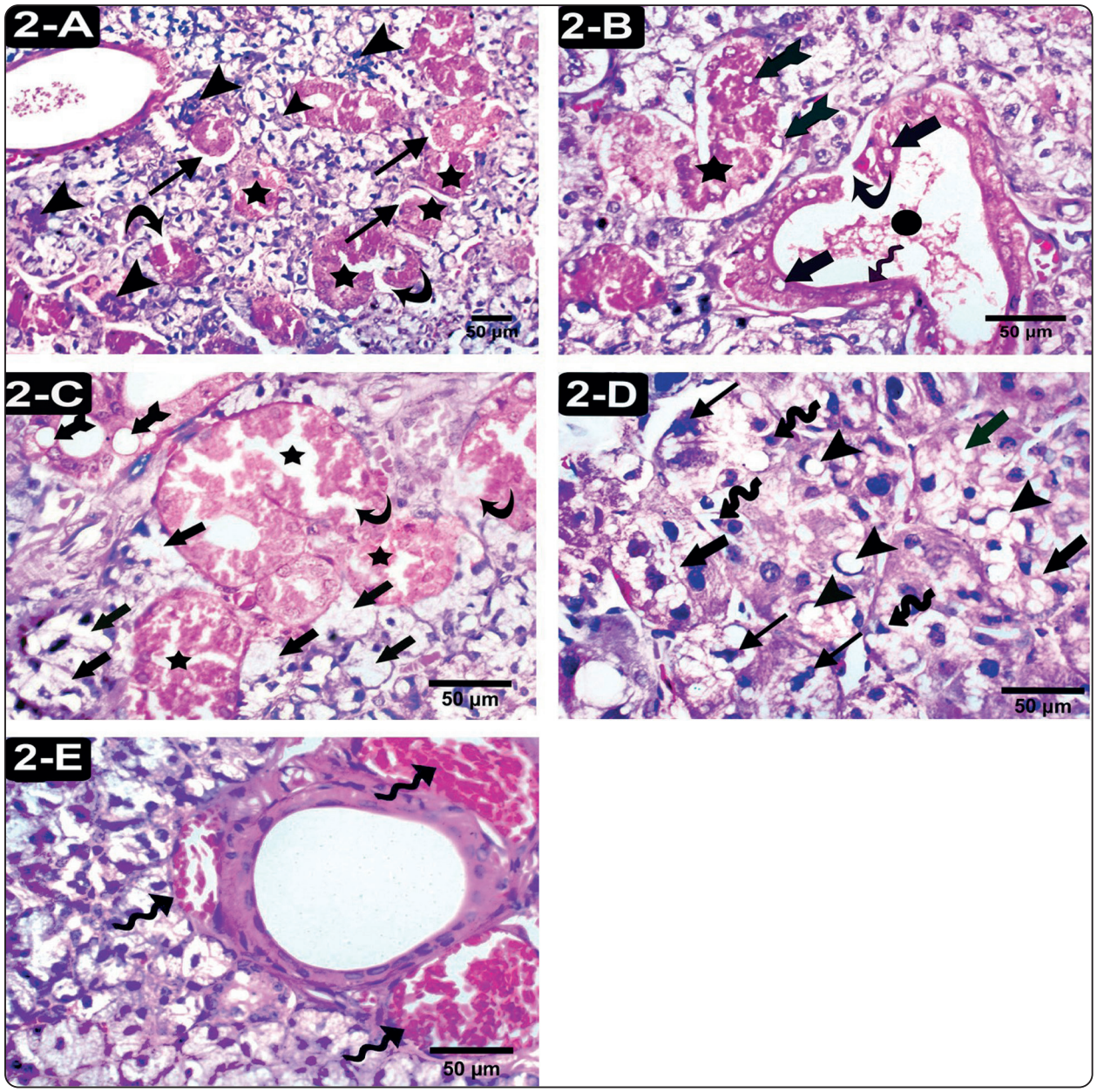

Fig. 2: (A, B, C, D & E) Photomicrographs of submandibular gland sections from group II (cisplatin group) showing: (A) Irregular shrunken acini (arrowheads) and disturbed granular ducts with clumping of their granular content (stars) and disruption of the basal cell membrane (curved arrows). Some ducts appear shrunken and surrounded by a space (thin arrows). (B) Dilated excretory duct with stagnant salivary secretion in its lumen (circle) and loss of the pseudo stratification of its lining epithelium with some nuclei appear flattened and apically displaced (wavy arrow), while others are karyolitic (thick arrows). Focal loss of the lining epithelium of the duct with discontinuity of the basement membrane is seen (curved arrow). Notice a distorted granular duct (star) with karyolysed nuclei (bifid arrows). (C) Acini with dark irregular or shrunken nuclei which are compressed by variable-sized cytoplasmic vacuoles occupying almost the whole cytoplasm (thick arrows), a striated duct with cytoplasmic vacuoles in the lining ductal cells (bifid arrows) and disturbed ducts (stars) that exhibit loss of their lining epithelium and disrupted basal cell membrane (curved arrows). (D) Loss of the normal acinar architectural features. Acini appear with vacuolated cytoplasm (thick arrows) and irregular (thin arrows), shrunken dark (wavy arrows) nuclei. Notice some acinar cells appear as signet rings (arrowheads). (E) Dilated congested blood vessels (wavy arrows).

(H&E X 200 A, X 400 B, C, D & E, Bar: 50 μm).

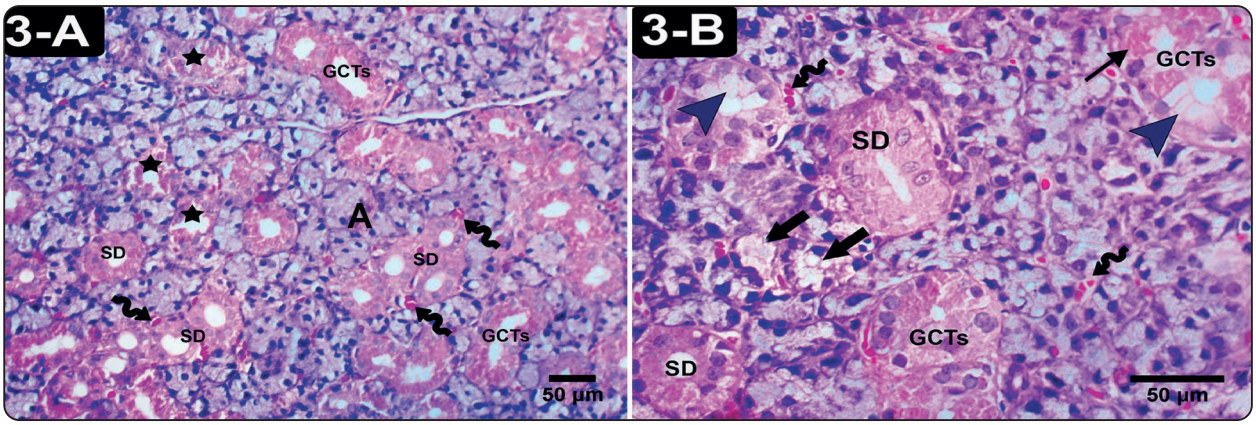

Fig. (3): (A&B) Photomicrographs of submandibular glands from group III (moringa oil+cisplatin group) showing: (A) Intralobular ducts (SD & GCTs) and acini (A) that appear more or less as the control group. Few ducts appear destructed (stars) with mild congestion of some blood capillaries (wavy arrows). (B) Almost normal striated ducts (SD) and granular ducts (GCTs) with few ductal cells appear with reduced acidophilic content (arrowheads) and clumped granular content in other ductal cells (thin arrow). Notice a few acini with vacuolated cytoplasm (thick arrows) and congested blood capillaries (wavy arrows). (H&E X 200A, X 400 B, Bar: 50 μm).

- Group IV (sesame oil + cisplatin group)

Administration of sesame oil with cisplatin ameliorated to great extent the histological changes induced by cisplatin. The submandibular gland appeared with histological architecture nearly similar to the control group. Densely packed serous acini with regular nuclei having symmetrical shape and size as well as normal ducts were seen. Nevertheless, there were minimal alterations noticed in some areas such as cytoplasmic vacuoles in a few acinar cells as well aa s few distorted ducts. Mild congestion in some blood capillaries was also noticed. (Fig. 4- A & B)

Periodic Acid Schiff's (PAS) staining

Positive PAS response manifested as a bright magenta hue, indicating the presence of glycoprotein and glycogen. In the control group (group I), PAS-stained tissue demonstrated a robust positive PAS reaction mostly in the basement membrane of the acini and ducts (Fig.5-A). In contrast, the CP group displayed a weakly positive PAS reaction and partial or total basement membrane degradation in some acini and ducts (Fig.5-B). In the MO+CP group, PAS-stained tissue demonstrated a moderate PAS-positive reaction in the acini and ducts with partial loss of the basement membrane in some ducts (Fig. 5C), whereas the SO+CP group demonstrated a strong PAS-positive reaction predominantly in the basement membrane of the acini and ducts (Fig.5-D).

Immunohistochemical results:

PCNA immunostaining

Immunohistochemical staining with PCNA demonstrated the proliferation in the nuclei of both acinar and ductal epithelial cells. The positive immunoreactivity for PCNA appeared in the form of brown colouration in the nuclei of the immunoreactive cells. The control group revealed strong +ve PCNA immunoreactivity in most of the acinar and ductal cellular nuclei (Fig.6-A). However, the CP group revealed minimal localized positive immune expression of PCNA in a few nuclei of acinar and ductal cells (Fig.6-B). On the other hand, the MO+CP group (Fig.6-C) and SO+CP group (Fig.6-D) manifested moderate PCNA immunoreactivity in some acinar and ductal cells.

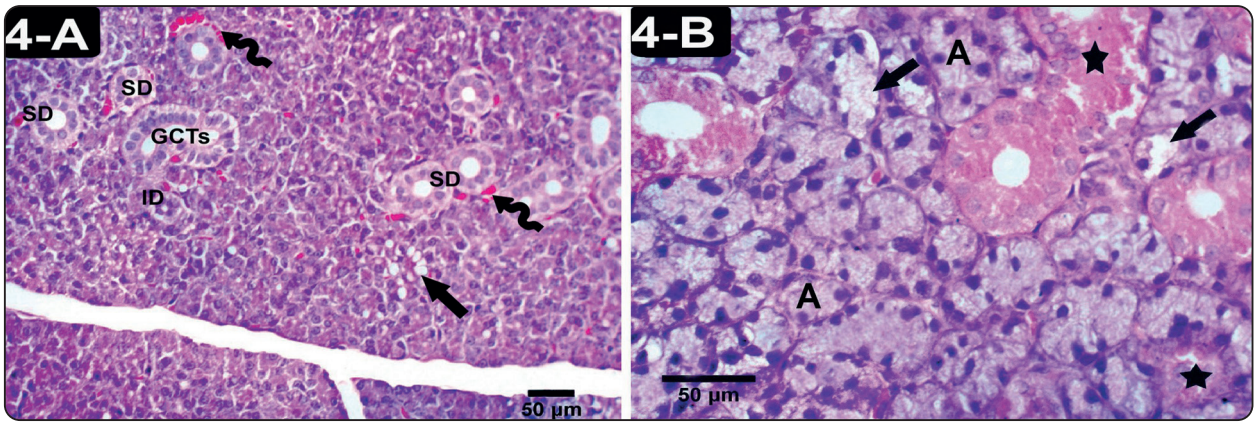

Fig. (4): (A&B) Photomicrographs of submandibular glands from group IV (sesame oil+cisplatin group) showing: (A) Acini and many intralobular ducts (ID, SD & GCTs) appear nearly as the control group with few acini show vacuolated cytoplasm and appear as signet ring (thick arrow) as well as mild congestion in the surrounded blood capillaries (wavy arrows). (B) Densely packed serous acini with regular nuclei (A), but few acini exhibit cytoplasmic vacuolation (thick arrows) and few ducts exhibit disturbed architecture (stars). (H&E X 200 A, X 400 B, Bar: 50 μm).

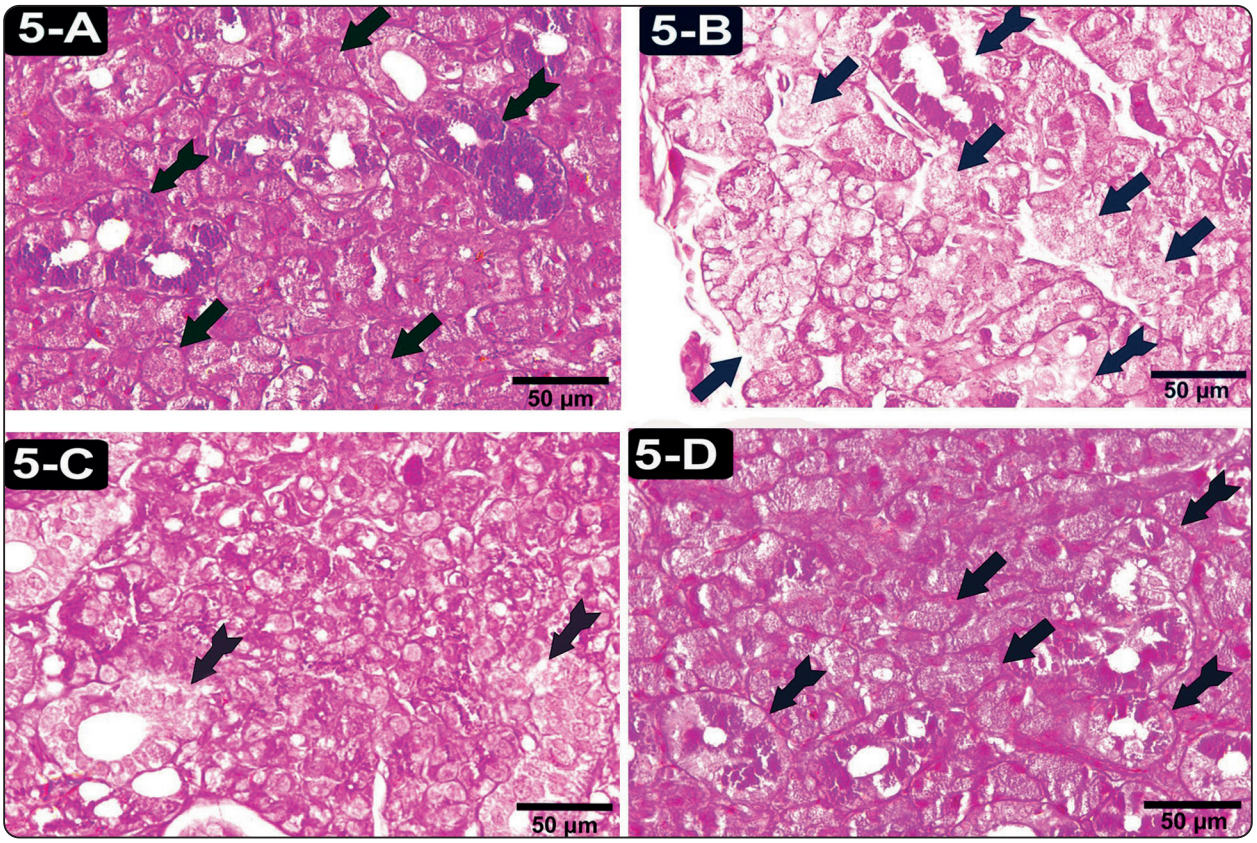

Fig. (5): Photomicrographs of PAS stained submandibular tissue of all studied groups Showing: (A) A strong positive PAS reaction mainly in the basement membrane of the acini (arrows) and ducts (bifid arrows) in the control group. (B) CP group shows weak positive PAS reaction and total or partial loss of the basement membrane in some acini (arrows) as well as in ducts (bifid arrows). (C) MO+CP group exhibits moderate PAS-positive reaction and partial loss of the basement membrane in some ducts (bifid arrows). (D) SO+CP group reveals a strong positive PAS reaction mainly in the basement membrane of the acini (arrows) and ducts (bifid arrows). (PAS stain X 400, Bar: 50 μm).

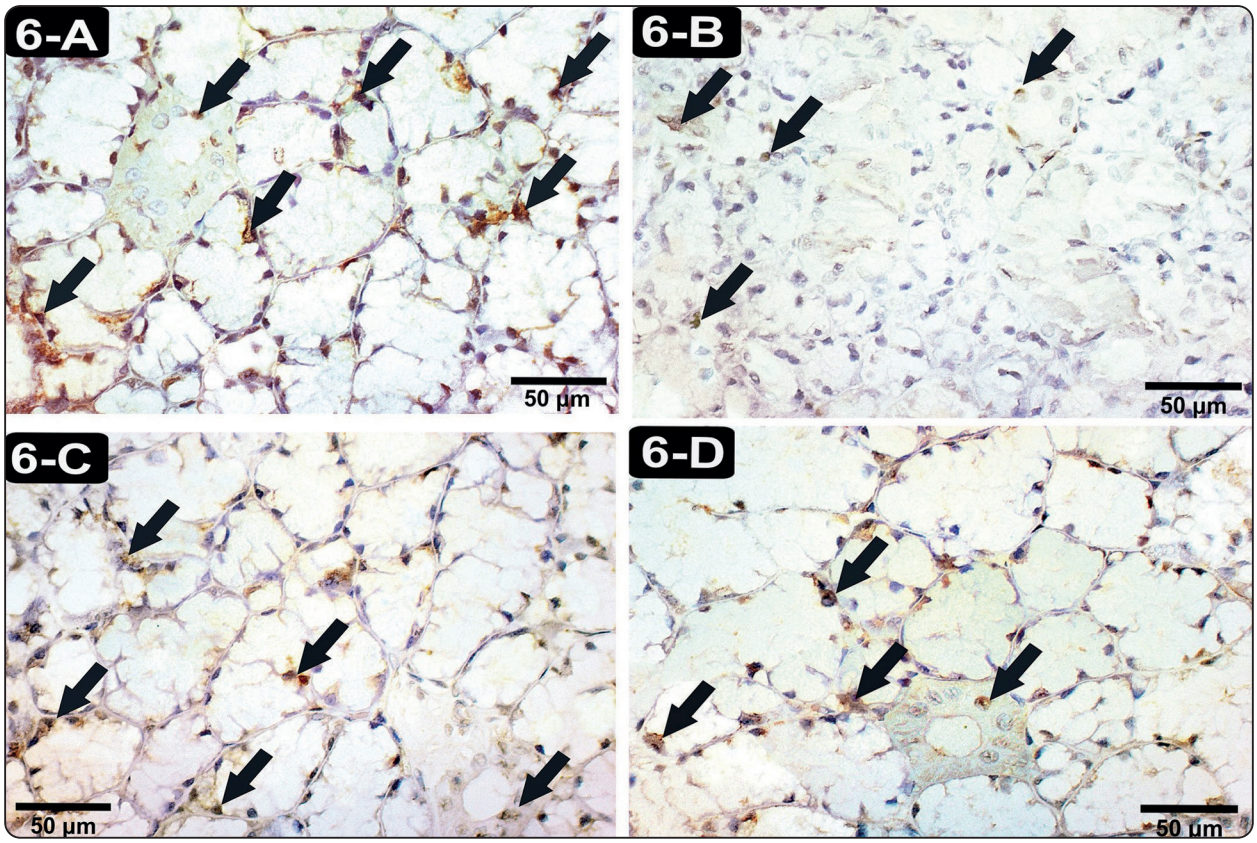

Fig. (6): Photomicrographs of PCNA stained submandibular tissue in all studied groups: (A) Showing strong +ve PCNA immunoreactivity in most of the acinar and ductal cellular nuclei in the control group (arrows). (B) Showing minimal localized +ve PCNA immunoreactivity in a few nuclei of acinar and ductal cells in the CP group (arrows). (C) Showing moderate positive PCNA immunoreaction (arrows) in the MO+CP group. (D) Showing moderate positive PCNA immunoreaction (arrows) in the SO+CP group. (PCNA immunostaining x 400, Bar: 50 μm)

Caspase-3 immunostaining

The degree of apoptosis was demonstrated by caspase-3 immunohistochemical staining as brown discolouration of the cytoplasm in the immunoreactive cells. The control group showed a weak localized positive caspase-3 reaction in a few acinar and ductal cells (Fig.7-A), while the e CP group showed a strong diffuse caspase-3 positive reaction in numerous acinar and ductal cells (Fig.7-B). MO+CP group manifested moderate caspase-3 immunoreactivity (Fig.7-C), whereas the SO+CP group revealed weak positive caspase-3 immune expression in some acinar and ductal cells (Fig.7-D).

α-SMA immunostaining

Regarding α-SMA immunoreaction, it demonstrated the degree of proliferation of myoepithelial cells surrounding the glandular acini & ducts and appeared as brown deposits in their cytoplasm. α-SMA immuno-stained sections of the control group showed weak positive immunoreaction in the cytoplasm of the myoepithelial cells (MECs) around some acini and ducts (Fig. 8-A). On the other hand, a strong positive immunoreaction was noticed around the acini and ducts in the CP group (Fig. 8-B). There was a moderate positive immunoreaction around the acini and duct the s in the MO+CP group (Fig. 8-C), and a weak positive α-immunoreactive in the MO+CP group (Fig. 8-D).

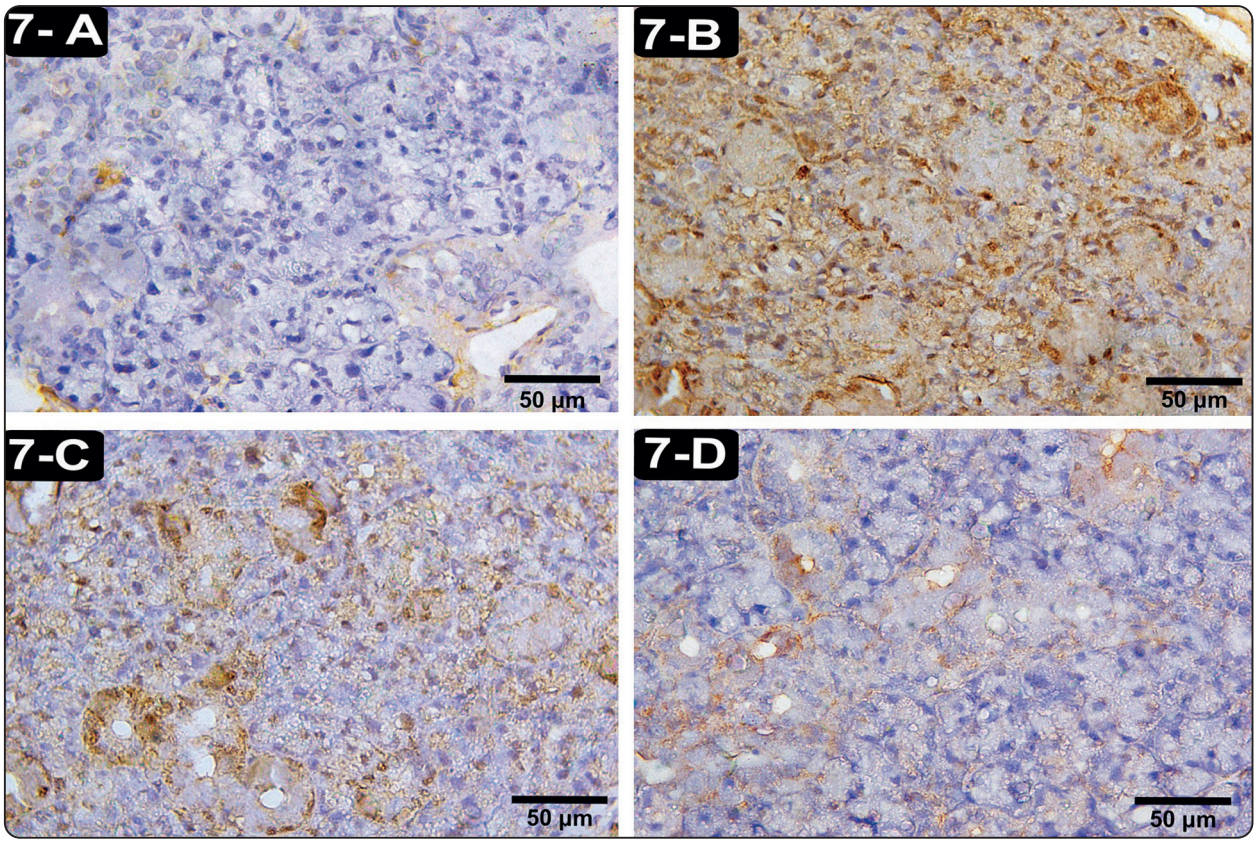

Fig. 7: Photomicrographs of caspase-3 stained submandibular tissues in all studied groups showing: (A) Weak localized caspase-3 immunoreactivity in the control group. (B) Strong diffuse +ve caspase-3 immunoreaction in the CP group. (C) Moderate +ve caspase-3 immunoreaction in MO+CP group. (D) Weak +ve caspase-3 immunoreaction in MO+CP group.

(Caspase-3 immunostaining x 400, Bar: 50 μm)

The statistical analysis of the morphometric results

1. Assessment of the mean diameter (µm) of the acini

The morphometric data demonstrated a significantly significant (P= 0.000) decrease in the mean diameter of the acini n the cisplatin group (24.019 ±3.53) in comparison to the control group(36.83±5.594) Yet, there was a highly significant increase (P= 0.000) in the mean acinar diameter in groups III and IV compared to the o cisplatin between group-group III and the control group, there was a significant decrease (P = 0.012), however, there was no significant difference (P = 0.257) between group IV and the control group. (Table-1; Graph-1a).

2. Assessment of the Mean Area % of (PAS, Caspase- 3, and α-SMA)

In terms of the mean area percentage of PAS, the cisplatin group demonstrated a significantly significant reduction (P= 0.000) (16.129±2.489) compared to the control group (26.211±1.2). In contrast, group III (24.997±2.419)and group IV(25.344±1.738) demonstrated a highly significant increase (P=0.000) in the area % of PAS compared to the cisplatin group. In contrast, there was a nonsignificant difference (P =0.147) between group IV and the control group, although the area % of PAS decreased significantly (P = 0.017) between group III and the control group. (Table-1; Histogram-1b)

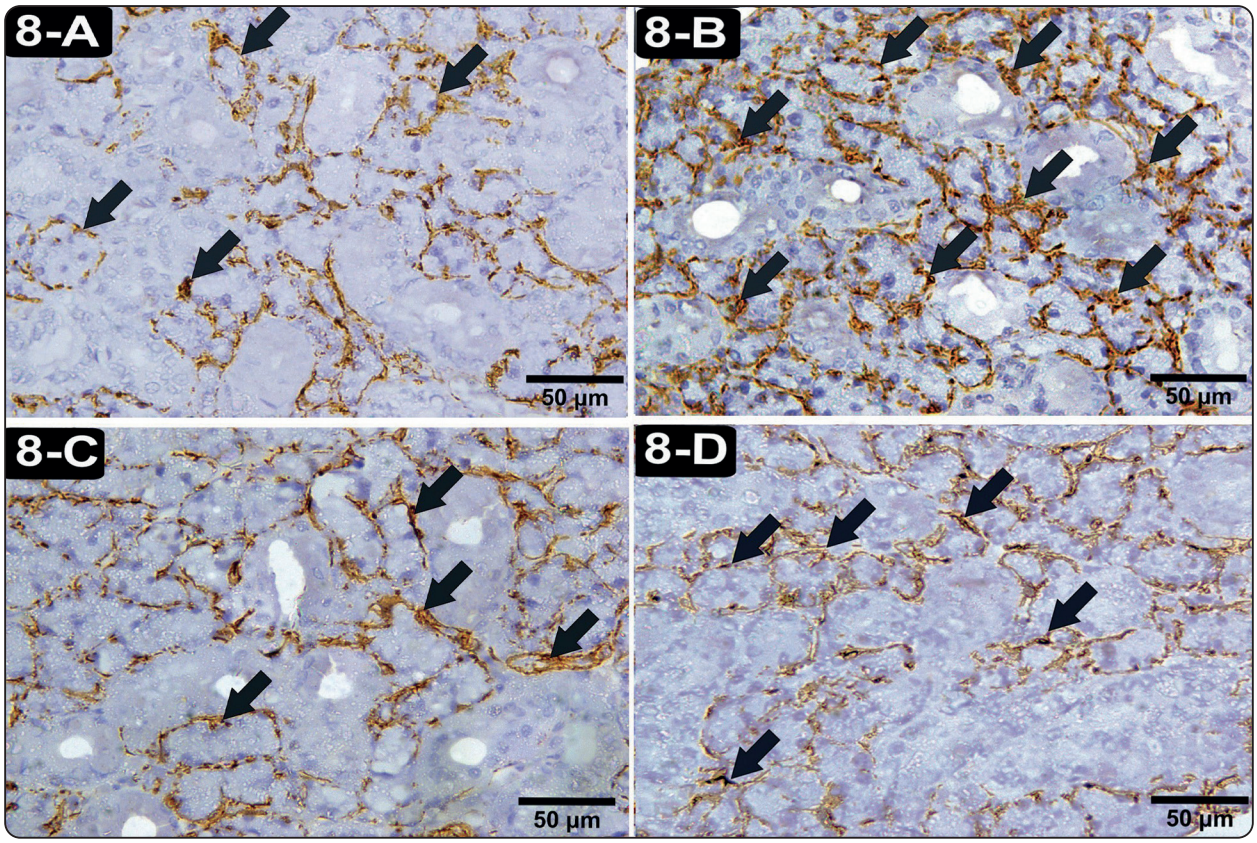

Fig. (8) A photomicrograph of α-SMA stained submandibular glands from all studied groups showing: (A) Weak positive α-SMA immunoreaction in the cytoplasm of the myoepithelial cells around ducts and acini (arrows) in the control group. (B) An apparent strong positive α-SMA immunoreaction in MECs (arrows) in the CP group. (C) Moderate positive immunoreaction for α-SMA (arrows) in the MO+CP group. (D) Weak positive immunoreaction for α-SMA (arrows) in the MO+CP group.

(α-SMA immunostaining x 400, Bar: 50 μm)

The mean area% of caspase-3 expression was significantly higher in the cisplatin group (13.054±0.666) than in the control group (1.925±0.125)(P= 0.000). Comparatively, the area % of caspase-3 in groups III (4.111±0.369) and IV (2.107±0.257)decreased by a significantly significant amount (P=0.000) as compared to the cisplatin group. There was a significantly significant increase in the area%of caspase-3 expression in group III compared to the control group (P= 0.000), however, there was no difference between group IV and the control group (P = 0.126). (Table-1 and Histogram-1c)-Statistical analysis revealed a highly significant increase (P = 0.000) in the area % of α-SMA in the cisplatin group (9.507± 1.842) as compared to that of the control group (5.687± 0.83). On the other hand, group III (6.328± 0.81) and group IV (6.157± 0.694) manifested a high significant decrease (P= 0.000) in the area % of α-SMA in comparison with the cisplatin group. Furthermore, there was a significant increase (P = 0.028) in the area % of α-SMA between group III and the control group, whereas there was a non-significant difference between group III (P = 0.171) versus the control group. (Table-1; Histogram-1d)

3. Assessments of the mean number percentage of PCNA-positive cells

Concerning the morphometrical analysis of the mean number percentage of PCNA positive cells in the cisplatin group (18.984±3.819) exhibited a highly significant decrease (P=0.000) as compared to that of the control group (25.89±4.945). Whereas group III (23.995±5.955) and group IV (24.049±4.984) manifested a highly significant increase (P= 0.000) in the mean number % of PCNA-positive cells in comparison with the cisplatin group. On the other hand, there was a non-significant difference between both groups III (P = 0.231) and IV (P = 0.255) versus the control group (I). (Table-1; Histogram-1e)

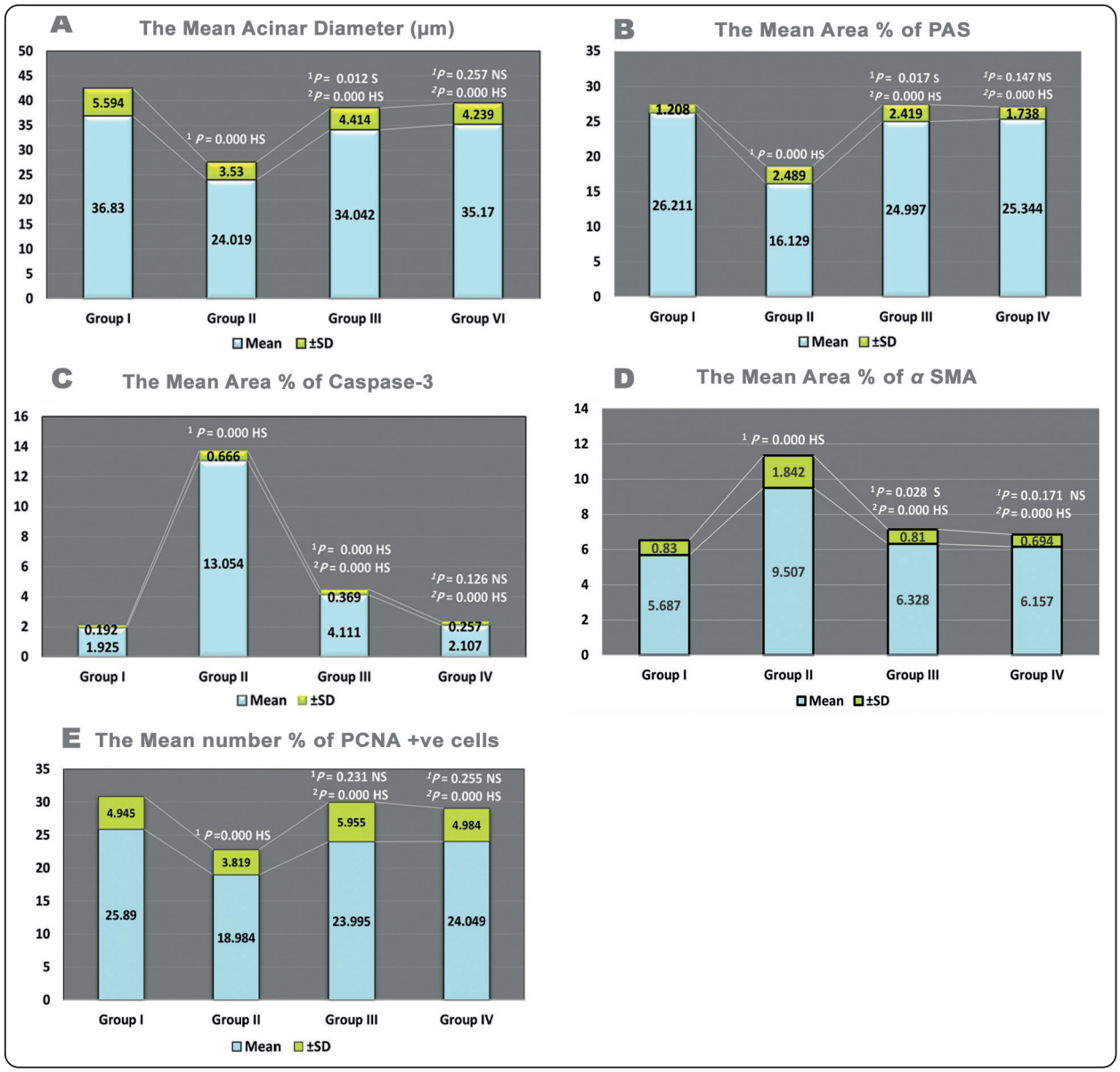

Histogram (1): shows (a) the mean acinar diameter (µm), (b) the mean area percentage of PAS stain, (c) the mean area percentage of caspase-3, (d) the mean area percentage of α-SMA, and (e) the mean number percentage of PCNA positive cells in all studied groups. (one-way ANOVA followed by Tukey's posthoc test was used). 1P: vs. control; 2P: vs. group II; HS: highly significant P ≤ 0.01; S: significant P ≤ 0.05; NS: non-significant P > 0.05.

TABLE (1): Mean ± SD of the mean acinar diameter (um) , the mean area % of (PAS , Caspase 3, alpha SMA) and the mean number % of PCNA +ve cells of all groups.

Mean ± SD P value /significance	Mean acinar diameter (um)	Area % of PAS	Area %of caspase 3	Area % of alpha SMA	Mean number % of PCNA +ve cells
GI	36.83 ±5.594	26.211 ±1.208	1.925 ±0.192	5.687 ±0.83	25.89 ±4.945
GII	24.019 ± 3.53 [1]P=0.000 HS	16.129 ±2.489 [1]P=0.000 HS	13.054 ± 0.66 [1]P=0.000 HS	9.507 ± 1.842 [1]P=0.000 HS	18.984 ± 3.819 [1]P=0.000 HS
GIII	34.042 ±4.414 [1]P=0.012 S [2]P=0.000 HS	24.997 ±2.419 [1]P=0.017 S [2]P=0.000 HS	4.111 ± 0.369 [1]P=0.000 HS [2]P=0.000 HS	6.32 ±0.81 [1]P=0.000 HS [2]P=0.000 HS	23.995 ±5.955 [1]P=0.028 S [2]P=0.000 HS
GIV	35.17 ±4.239 [1]P=0.257 NS [2]P=0.000 HS	25.344 ±1.738 [1]P=0.147 NS [2]P=0.000 HS	2.107 ± 0.257 [1]P=0.126 NS [2]P=0.000 HS	6.157 ± 0.694 [1]P=0.171 NS [2]P=0.000 HS	24.049 ±4.984 [1]P=0.255 NS [2]P=0.000 HS

[1]P vs control ; [2]P vs GII (HS highly significant P≤0.01 ; S: significant P≤0.05; NS: non-significant P> 0.05)

DISCUSSION

The current investigation aimed to evaluate the effects of CP on the anatomy of the submandibular glands and to compare the efficacy of MO and SO as possible ameliorative conjugant therapies. The goals of this investigation were to evaluate the effects of CP on the anatomy of the submandibular glands. In this case, CP is frequently used as an effective chemotherapeutic medication for treating a wide variety of cancers. By attaching to cellular DNA (Cepeda et al., 2007) or mitochondrial DNA (Li et al., 2006), CP can trigger cytotoxic changes that ultimately result in apoptosis or programmed cell death (Li et al., 2006). (Li et al., 2006). (Fuertes et al., 2003). In addition to this, it promotes the production of reactive oxygen species, which, in turn, leads to an increase in lipid peroxidation and Ca2+ influx, both of which might result in apoptosis (Casares et al., 2012).

Comparing the CP group to the control group, the CP group's ducts and acini displayed significant structural changes. Their nuclei were black, irregular, or karyolysis and their acini and ducts were irregular, shrunken, and malformed. In addition, vacuolated cytoplasm, localised loss of the lining epithelium and basement membrane, and a decrease in the average acinar diameter were observed. The statistical analysis of acinar diameter revealed that the CP group's acinar diameters were significantly smaller than those of the control group. Similar alterations were detected in the submandibular glands of cisplatin-treated rats by Kitashima (2005) and Amin and Fathy (2017). Its potential to induce oxidative stress, followed by the accumulation of reactive oxygen species and lipid peroxidation, promotes severe cytotoxic effects via the opening of the permeability transition pore complex (Elgamily and Denewar, 2020).

Concerning the partial or total loss of the lining epithelium and basement membrane of ducts and acini in the CP group, it was confirmed by the morphometric study followed by the statistical analysis of the area% of PAS stain, as the CP group displayed a weak positive PAS reaction and partial or total loss of the basement membrane in ducts. Dasari and Tchounwou (2014) noted that lipid peroxidation is the initial indication of oxidative damage induced by ROS and that the cell membrane is the first line of defence against these free radicals before other cellular components are susceptible to oxidative modification and damage.

According to Satoh and Yoshihara (2004), the occurrence of intracytoplasmic vacuoles may be due to the membranes of neighbouring secretory granules combining to form intracytoplasmic vacuoles. Moreover, according to Amin and Fathy (2017), the free radicals created by CP harm the cellular components. Kassab and Tawfik (2018) found that cytoplasmic vacuolation may have resulted from a decrease in the secretory activity of the acinar cells, which in turn leads to a decrease in the secretory content of the granules. Moreover, certain acinar cells in the CP group resemble signet rings. Elgamily and Denewar (2020) interpreted this finding and explained that it may be caused by multiple variable-sized cytoplasmic vacuoles that occupy nearly the entire cytoplasm, causing compression and displacement of the nuclei from their normal positions, resulting in the crescent or signet ring appearance.

According to Hany et al., the dark, shrunken, pyknotic nuclei with an irregular contour in the ducts and acini of the submandibular gland in the CP group can be attributed to the CP effect on the nucleus, which causes DNA plastination and cytotoxic alterations that may result in apoptosis (2017). Comparing the CP group to all other groups, our statistical analysis demonstrated a significant increase in the area percentage of caspase-3 in the CP group. This observation was made by Elgamily and Denewar (2020) in parotid glandcisplatin-treated rats. They explained that cisplatin is displaced by water molecules that replace the chloride atoms on cisplatin, resulting in a hydrolyzed compound that can react with any nitrogen donor atom on the nucleic acid, resulting in DNA damage that inhibits cell division and causes non-selective apoptosis that affects both.

Regarding the PCNA immunohistochemical staining in the current study, the statistical analysis revealed a highly significant decrease in positive immune expression of PCNA compared to other groups which indicate a decrement in the proliferation of both acinar and ductal epithelial cells. These results come in agreement with another study performed by **Mubarak and Ali (2012)** while concerning the proliferation index by PCNA, ***the*** CP group showed decreased proliferation capacity as compared the to control group which could be explained by deteriorated tissue architecture and function as reported by **Hany et al. (2017).** Another study by **Terzi et al. (2017)** interpreted that finding by the ability of cisplatin to minimize saliva production either by blocking the aquaporin expression or by stabilizing DNA strands which in turn prevents the regeneration and proliferation of the glandular tissue because of progenitor cells' damage.

As regard the α-SMA immunostaining, this immune reaction showed the degree of the myoepithelial cell (MECs) proliferation (**El Sadik et al., 2018)**. MECs, in normal circumstances, line the periphery of the acini and ducts in salivary glands and surround them with their processes (**Ayuob et al., 2019).** In the current study, a highly significant increase in the area % of α-SMA was statistically proved in the cisplatin group as compared to all other groups. This revealed that cisplatin affected the structural integrity of MECs around both acini and ducts. Such findings support other previous studies as **Abdel-Daim et al. (2017)** and **Maghmomeh et al. (2020)** who noticed increased α-SMA protein levels in the kidney of cisplatin-treated rats as well as **Nasralla and Mogeda (2018)** who recorded an increase in α-SMA expression in the myocardium of cisplatin-treated rats. **Mousa (2011)** explained that the morphological and proliferative changes of MECs occur during the atrophy and regeneration of acinar cells, as in a parenchymal injury, with subsequent increase in their size and number to increase the secretory function of these cells. Moreover, **Kassab and Tawfik (2018**) stated that the active proliferation of MECs increased by two folds in the acinar cells, four folds in ductal cells and ten folds in the myoepithelial cells during pathological conditions.

Dilated congested blood vessels that were noticed in this study agree with the findings of **Zahawi (2015)** in SMG of rabbits after receiving chemotherapy and he attributed such dilatation and congestion to inflammatory reaction associated with chemotherapy treatment which increases trans-endothelial permeability.

The proposed mechanisms by which natural known antioxidants may improve organ functions have been investigated over a long period. Moringa Oleifera (MO) is a popular element in traditional medicine that has various types of antioxidant compounds such as ascorbic acid, flavonoids, phenolics, anthocyanins, and carotenoids. Free radical scavenging activity is one of the important antioxidant properties because of the deleterious role of free radicals. **(Abdulkarim et al., 2005; Alhakmani et al., 2013; Vongsak et al., 2014).**

In the present investigation, the administration of moringa oil concurrently with cisplatin decreased the pathological changes generated by CP, as evidenced by the presence of fewer acini with cytoplasmic vacuolation and fewer destructed ducts, as well as mildly congested blood capillaries. These findings are consistent with those of Moawad et al. (2016), who demonstrated that moringa oleifera extract protected the parotid gland against the effects of cisplatin. The decreased incidence of vacuolation in the acini and ductal system compared to the cisplatin group is consistent with the findings of Al Shammari and El-Mehiry (2016) on the effects of moringa against the adverse effects of cisplatin in the kidneys of rats. The researchers concluded that the antioxidant effect of moringa plays a significant role in reducing cisplatin-induced renal damage. In addition, the treatment with moringa oil lowered blood cholesterol, LDL cholesterol, and TG levels. Thus, it is probable that moringa oil extract lowered tissue lipid accumulation and vacuolation. Hence, our finding validated the researchers' conclusions that moringa oil may be administered concomitantly with the chemotherapeutic treatment as cisplatin to minimize its toxicity.

The decrease in degenerative changes and congestion of blood vessels in rats treated with moringa (group III) coincides with the findings of Mahajan et al. (2007), who discovered that with treatment with an ethanolic extract of M. oleifera seeds, there was a significant decrease in oedema and congestion, serum levels of inflammatory mediators, and lymphocytic infiltration. In the present investigation, when MO oil was co-administered with cisplatin, the decrease in PCNA expression and the increase in caspase-3 & -SMA expression found in the CP group were significantly mitigated. As stated by Mahran et al., this ameliorative effect may be attributable to the components of MO oil (tocopherols, oleic and linoleic fatty acids) (2022). Moreover, Famurewa et al. (2019); Edeogu et al. (2020) and Abdel-Daim et al. (2020) explained that moringa oil can inhibit the activation of caspase-3 signalling due to its antioxidant capacity by restoring the activity of antioxidant molecules and decreasing the levels of pro-oxidant molecules, as well as due to its tocopherols and sterols content, which have anti-apoptotic effects Higher PCNA expression in the MO+CP group is consistent with what Bin-Meferij and El-Kott (2015) observed in the testes of moringa-treated rats exposed to electromagnetic radiation. They attributed this impact to the high antioxidant content of moringa, which may inhibit the first mediation of apoptosis by reactive oxygen species (ROS). In addition, Supriono et al. (2020) revealed that moringa oleifera inhibits -smooth muscle actin to reduce -SMA expression in the liver.

Sesame oil was chosen in this study because it contains potent polyphenolic antioxidants (sesamin, sesamol, sesamolin, and -tocopherol) that can protect against oxidative stress and contribute to sesame oil's antioxidant function (Shuang et al., 2018; Zhang et al., 2016a). Moreover, Radi et al. (2019) reported that sesame oil possesses anti-inflammatory, antimicrobial, hypolipidemic, and anticancer properties. Sankar et al. (2005) confirmed that sesame oil provides superior protection against lipid peroxidation compared to other dietary oils via regulating in vivo antioxidants.

Submandibular glands appeared reasonably normal, with densely packed serous acini and regular nuclei of symmetrical shape and size, as well as virtually normal ducts, except for a few twisted ducts and cytoplasmic vacuoles in a few acinar cells, as determined by the current study. This may be evidence of SO's antioxidant properties. Our results concur with those of Ali et al. (2020), whose findings indicated that sesame had ameliorated CP-induced nephrotoxicity in rats by reversing CP-induced oxidative stress. The researchers concluded that sesamin at a modest dose was efficient in counteracting the adverse effects of cisplatin, confirming its potent antioxidant properties.

Moreover, our results are consistent with those of Meng et al. (2017), Ali et al. (2020), and Dilek et al. (2020), who reported that among the mechanisms involved in sesamin amelioration of cisplatin-induced nephrotoxicity was a significant reduction in lipid peroxidation, oxidative and nitrosative stress, apoptosis, and inflammation. Hsu et al. (2007) suggested that sesame oil mitigated cisplatin-induced hepatic and renal damage by decreasing nitric oxide-associated lipid peroxidation and reported that sesame oil may play a significant role in avoiding cisplatin-induced multiple organ damage during chemotherapy.

In the SO-treated group, the significant reduction in PCNA expression and the elevation in caspase-3 & -SMA expression observed in the CP group essentially recovered to normal levels. Hsu et al. (2007) revealed that sesame oil decreased cisplatin-induced hepatic and renal damage, as well as cisplatin-initiated lipid peroxidation and the formation of hydroxyl radicals, without altering the anticancer activity of cisplatin. Zhang et al. (2016 b) observed a decrease in SMA expression in the kidneys of rats exposed to dyslipidemia and treated with sesame oil; sesame downregulated -SMA expression. Hamoud and Radwan (2019) discovered a decrease in caspase 3 expression in injured skeletal muscles treated with sesame oil, which is consistent with the drop observed in the SO+CP group. They attributed this discovery to the potent potential of sesame oil to reduce oxidative stress, inflammation, and apoptosis. Concerning the increased PCNA expression in the SO+CP group compared to the CP group, this is consistent with the findings of Valacchi et al. (2013), who observed that mice treated with sesame oil had a faster rate of wound closure as well as an increased n PCNA levels, indicating an increase in cellular proliferation.

In the current study, treatment of rats with moringa oleifera oil or sesame oil concurrently with cisplatin significantly mitigated the cisplatin-induced oxidative stress and tissue damage, but this ameliorating effect was more apparent in the sesame oil-treated group than in the moringa oil-treated group. This was proved by a statistical evaluation of the morphometric results. Although both groups demonstrated a high statistically significant difference in all morphometric measurements compared to the CP group, the moringa-treated group demonstrated a significant decrease in the mean acinar diameter and the area% of PAS, and an increase in the area% of caspase-3 and -SMA, compared to to the control group. In contrast, the sesame group and the control group did not differ significantly on any of these metrics, which were virtually within the normal range.

CONCLUSIONS

Both moringa oil and sesame oil were beneficial in mitigating unfavourable effects produced by cisplatin treatment in the submandibular salivary glands of albino rats, with moringa oil showing a modest advantage over sesame oil. Based on these findings, future research into the efficacy of natural product extracts as potential preventive agents against chemotherapy adverse effects is possible. Enhancing our understanding of the process requires additional research into the molecular mechanism(s) of the positive effects of both oils. the precise mechanism through which each oil produced these benefits.

Competing interests:

The authors declare that they have no conflict of interest.

REFERENCES

1. Abdel-Daim MM, Alkahtani S, Almeer R, Albasher G. Alleviation of lead acetate-induced nephrotoxicity by Moringa oleifera extract in rats: highlighting the antioxidant, anti-inflammatory, and anti-apoptotic activities. Environmental Science and Pollution Research. 2020 Sep;27(27):33723-31.
2. Abdel-Daim MM, El-Sayed YS, Eldaim MA, Ibrahim A. Nephroprotective efficacy of ceftriaxone against cisplatin-induced subchronic renal fibrosis in rats. Naunyn-Schmiedeberg's archives of pharmacology. 2017 Mar;390(3):301-9.
3. Abdel-Latif HM, Abdel-Daim MM, Shukry M, Nowosad J, Kucharczyk D. Benefits and applications of Moringa oleifera as a plant protein source in Aquafeed: A review. Aquaculture. 2022 Jan 30;547:737369.
4. Abdulkarim SM, Long K, Lai OM, Muhammad SK, Ghazali HM. Some physicochemical properties of Moringa oleifera seed oil extracted using solvent and aqueous enzymatic methods. Food chemistry. 2005 Nov 1;93(2):253-63.
5. Abdulmonem AM. Histological and immunohistochemical study to evaluate the effects of chamomile versus green tea extracts on the salivary glands of methotrexate-treated male albino rats (Doctoral dissertation, Fayoum University). Nat Sci. 2020;18(1):74-95.
6. Al Shammari A, El-Mehiry H. Amelioration of cisplatin-induced sexual toxicity on male rats by using fortified flat read with moringa oleifera. Bulletin of the National Nutrition Institute of the Arab Republic of Egypt. 2016 Nov 1;47(2):1-29.
7. Alhakmani F, Kumar S, Khan SA. Estimation of total phenolic content, in–vitro antioxidant and anti–inflammatory activity of flowers of Moringa oleifera. Asian Pacific journal of tropical biomedicine. 2013 Aug 1;3(8):623-7.
8. Ali BH, Al Salam S, Al Suleimani Y, Al Za'abi M, Ashique M, Manoj P, Sudhadevi M, Al Tobi M, Nemmar A. Ameliorative effect of sesamin in cisplatin-induced nephrotoxicity in rats by suppressing inflammation, oxidative/nitrosative stress, and cellular damage. Physiol. Res. 2020 Feb 1;69(1):61-72.
9. Amin LE, Fathy H. Role of Ghrelin on cisplatin-induced morphological changes on submandibular salivary glands. Egyptian Dental Journal. 2017 Oct 1;63(4-October (Oral Medicine, X-Ray, Oral Biology & Oral Pathology)):3225-33.
10. Antunes LM, DARIN JD, Bianchi MD. Protective effects of vitamin C against cisplatin-induced nephrotoxicity and lipid peroxidation in adult rats: a dose-dependent study. Pharmacological research. 2000 Apr 1;41(4):405-11.
11. Ayuob NN, Abdel-Tawab HS, El-Mansy AA, Ali SS. The protective role of musk on salivary glands of mice exposed to chronic unpredictable mild stress. Journal of oral science. 2019; 61(1):95-102.
12. Beloucif A, Kechrid Z, Bekada AM. Effect of zinc deficiency on blood glucose, lipid profile, and antioxidant status in streptozotocin-diabetic rats and the potential role of sesame oil. Biological Trace Element Research. 2021 Oct 6:1-2.
13. Bin-Meferij MM, El-Kott AF. The radioprotective effects of Moringa oleifera against mobile phone electromagnetic radiation-induced infertility in rats. International Journal of Clinical and Experimental Medicine. 2015;8(8):12487.
14. Buchwalow IB, Böcker W. Working with antibodies. In: immunohistochemistry: basics and methods. Springer Berlin Heidelberg. 2010:31–9.
15. Casares C, Ramírez-Camacho R, Trinidad A, Roldán A, Jorge E, García-Berrocal JR. Reactive oxygen species in apoptosis induced by cisplatin: a review of physiopathological mechanisms in animal models. Eur Arch Otorhinolaryngol. 2012; 269:2455-2459.
16. Cepeda V, Fuertes MA, Castilla J, Alonso C, Quevedo C, Pérez JM. Biochemical mechanisms of cisplatin cytotoxicity. Anti-Cancer Agents in Medicinal Chemistry (Formerly Current Medicinal Chemistry-Anti-Cancer Agents). 2007 Jan 1;7(1):3-18.
17. Dasari S, Tchounwou PB. Cisplatin in cancer therapy: molecular mechanisms of action. European journal of pharmacology. 2014 Oct 5; 740:364-78.
18. Dawson B, Trapp RG. Basic & Clinical Biostatistics.: In Basic & Clinical Biostatistics. 4th ed. Lange Medical Books / McGraw-Hill Medical Publishing Division; 2004:162–89.

19. Dilek ME, Gurel A, Dogantekin A, Sahin K, Hanifi I, Ozercan, Ilhan N, HKafkas. Effects of sesamol on experimental cisplatin nephrotoxicity. Model J Med Sci. 2020; 10(3):180–187 doi: 10.5505/kjms.2020.54227

20. Edeogu CO, Kalu ME, Famurewa AC, Asogwa NT, Onyeji GN, Ikpemo KO. Nephroprotective effect of Moringa oleifera seed oil on gentamicin-induced nephrotoxicity in rats: biochemical evaluation of antioxidant, anti-inflammatory, and antiapoptotic pathways. Journal of the American college of nutrition. 2020 May 18;39(4):307-15.

21. El Sadik A, Mohamed E, El Zainy A. Postnatal changes in the development of rat submandibular glands in offspring of diabetic mothers: Biochemical, histological and ultrastructural study. PLoS One. 2018 Oct 10;13(10): e0205372.

22. Elgamily MF, Denewar M. Potential benefit of Annona muricata extract in combating cisplatin-induced injury of the parotid gland in albino rats. Egyptian Dental Journal. 2020 Apr 1;66(2-April (Oral Medicine, X-Ray, Oral Biology & Oral Pathology):997-1007.

23. Famurewa AC, Asogwa NT, Aja PM, Akunna GG, Awoke JN, Ekeleme-Egedigwe CA, Maduagwuna EK, Folawiyo AM, Besong EE, Ekpono EU, Nwoha PA. Moringa oleifera seed oil modulates redox imbalance and iNOS/NF-κB/caspase-3 signalling pathway to exert antioxidant, anti-inflammatory and antiapoptotic mechanisms against anti-cancer drug 5-fluorouracil-induced nephrotoxicity in rats. South African Journal of Botany. 2019 Dec 1; 127:96-103.

24. Fan D, Yang Z, Liu FY, Jin YG, Zhang N, Ni J, Yuan Y, Liao HH, Wu QQ, Xu M, Deng W. Sesamin protects against cardiac remodelling via Sirt3/ROS pathway. Cellular Physiology and Biochemistry. 2017 a; 44(6):2212-27.

25. Fan D, Yang Z, Yuan Y, Wu QQ, Xu M, Jin YG, Tang QZ. Sesamin prevents apoptosis and inflammation after experimental myocardial infarction by JNK and NF-κB pathways. Food & function. 2017 b;8(8):2875-85.

26. Fu X, Su J, Hou L, Zhu P, Hou Y, Zhang K, Li H, Liu X, Jia C, Xu J. Physicochemical and thermal characteristics of Moringa oleifera seed oil. Advanced Composites and Hybrid Materials. 2021 Sep;4(3):685-95.

27. Fuertes MA, Castilla J, Alonso C, Pérez JM. Cisplatin biochemical mechanism of action: from cytotoxicity to induction of cell death through interconnections between apoptotic and necrotic pathways. Curr Med Chem 2003; 10:257-266.

28. Gamble M. The Hematoxylins and Eosin. In: Bancroft, JD and Gamble M, editor. Theory and Practice of Histological Techniques. 6th ed. Philadelphia: Churchill Livingstone Elsevier; 2008:121–34.

29. Guo Q, Jin L, Li ZA, Huang GW, Liu HM, Qin Z, Wang XD, Ma YX. Sequential extraction, preliminary characterization and functional properties of sesame (Sesamum indicum L.) hull polysaccharides. LWT. 2022 Jun 13:113661.

30. Hamoud A, Radwan R. The possible protective role of sesame oil on skeletal muscle regeneration in induced red-bull injury: an experimental study. Journal of Medical Histology. 2019 Dec 1;3(2):216-24.

31. Hany E, Sobh MA, Abou ElKhier MT, ElSabaa HM, Zaher AR. The effect of different routes of injection of bone marrow mesenchymal stem cells on parotid glands of rats receiving cisplatin: a comparative study. International journal of stem cells. 2017 Nov;10(2):169.

32. Hsu DZ, Chen KT, Lin TH, Li YH, Liu MY. Sesame oil attenuates cisplatin-induced hepatic and renal injuries by inhibiting nitric oxide-associated lipid peroxidation in mice. Shock. 2007 Feb 1;27(2):199-204.

33. Hussein SI. Influence of intramasseteric injection of botulinum toxin types A on the Ipsilateral submandibular salivary gland of albino rats. Egyptian Journal of Histology. 2020 Sep 1;43(3):863-77.

34. Janaki S, Yamuna Devi P. Extraction of cold press Moringa oil. International Journal of Current Research. 2015 April;7(04): 14956-14957.

35. Kassab AA, Tawfik SM. Effect of a caffeinated energy drink and its withdrawal on the submandibular salivary gland of adult male albino rats: A histological and immunohistochemical study. Egyptian Journal of Histology. 2018 Mar 1;41(1):11-26.

36. Kheirati Rounizi S, Akrami Mohajeri F, Moshtaghi Broujeni H, Pourramezani F, Jambarsang S, Kiani H, Khalili Sadrabad E. The chemical composition and heavy metal content of sesame oil produced by different methods: a risk assessment study. Food Science & Nutrition. 2021 Jun;9(6):2886-93.

37. Kitashima S. Morphological alterations of submandibular glands caused by cisplatin in the rat. The Kurume medical journal. 2005;52(1+ 2):29-38.

38. Köroğlu KM, Çevik Ö, Şener G, Ercan F. Apocynin alleviates cisplatin-induced testicular cytotoxicity by regulating oxidative stress and apoptosis in rats. Andrologia. 2019 May;51(4):e13227.

39. Kostadinović Veličkovska S, Brühl L, Mitrev S, Mirhosseini H, Matthäus B. Quality evaluation of cold-pressed edible oils from Macedonia. European journal of lipid science and technology. 2015 Dec;117(12):2023-35.

40. Li XB, Schluesener HJ. Therapeutic effects of cisplatin on rat experimental autoimmune encephalomyelitis. Arch Immunol Ther Exp (Warsz) 2006; 54:51-53.

41. Maghmomeh AO, El-Gayar AM, El-Karef A, Abdel-Rahman N. Arsenic trioxide and curcumin attenuate cisplatin-induced renal fibrosis in rats through targeting Hedgehog signalling. Naunyn-Schmiedeberg's Archives of Pharmacology. 2020 Mar;393(3):303-13.

42. Mahajan SG, Mali RG, Mehta AA. Protective effect of ethanolic extract of seeds of Moringa oleifera Lam. against inflammation associated with the development of arthritis in rats. Journal of Immunotoxicology. 2007 Jan 1;4(1):39-47.

43. Mahran HA, Okdah YA, Zaky AA, Arisha SM. The possible ameliorative role of Moringa oleifera seed oil on sofosbuvir-induced nephrotoxicity in albino rats; histopathological, immunohistochemical and biochemical studies. The Journal of Basic and Applied Zoology. 2022 Dec;83(1):1-2.

44. Meng H, Fu G, Shen J, Shen K, Xu Z, Wang Y, Jin B, Pan H. Ameliorative effect of daidzein on cisplatin-induced nephrotoxicity in mice via modulation of inflammation, oxidative stress, and cell death. Oxidative medicine and cellular longevity. 2017 Oct; 2017.

45. Mili A, Das S, Nandakumar K, Lobo R. A comprehensive review on Sesamum indicum L.: Botanical, ethnopharmacological, phytochemical, and pharmacological aspects. Journal of Ethnopharmacology. 2021 Dec 5; 281:114503.

46. Moawad AAR, Mohammed MA, Ibrahim FM, Zaher FA. Biological impact of moringa oleifera extract on the parotid gland of cisplatin-induced renal failure in albino rats. Int. J. Adv. Res. 2016; 4(11): 1620-1627.

47. Mousa AM. Effect of sodium fluoride with and without ginseng on the submandibular gland of the adult male albino rat: a histological and immunohistochemical study. The Egypt J Histol 2011; 34:291–301.

48. Mubarak R, Ali ZH. Protective effects of L-Carnitine on Cisplatin-induced toxicity in rat parotid salivary glands. J Am Sci. 2012; 8(2): 137-14.

49. Nasralla M, Mogeda M. Possible prophylactic role of Querctine on Cisplatin-Induced myocardial toxicity in adult male albino rat: a histological and immunohistochemical study. The Medical Journal of Cairo University. 2018 Mar 1;86(March):395-403.

50. Ojima T, Nakamura M, Nakamori M, Katsuda M, Hayata K, Maruoka S, Shimokawa T, Yamaue H. Phase I/II trial of chemotherapy with docetaxel, cisplatin, and S-1 for unresectable advanced squamous cell carcinoma of the oesophagus. Oncology. 2018; 95:116-20.

51. Radi AM, Mohammed ET, Ibrahim Abushouk A, Lotfi Aleya AD. Modulatory effects of sesame oil and ascorbic acid on abamectin-induced oxidative stress in rat liver and brain tissues. Science of The Total Environment. 2019 Nov;134882.

52. Sankar D, Sambandam G, Rao MR, Pugalendi KV. Modulation of blood pressure, lipid profiles and redox status in hypertensive patients taking different edible oils. Clinica chimica acta. 2005 May 1;355(1-2):97-104.

53. Satoh M, Yoshihara T. Clinical and ultra cytochemical investigation of sialadenosis. Acta oto-laryngologica. Supplementum. 2004 Aug 1(553):122-7.

54. Shuang D, Zhou J, Fang H, Nie Z, Chen S, Peng H. Sesamin protects the femoral head from osteonecrosis by inhibiting ROS-induced osteoblast apoptosis in a rat model. Frontiers in physiology. 2018; 9: 1787.

55. Supriono S, Kalim H, Permatasari N, Susianti H. Moringa oleifera inhibits liver fibrosis progression by inhibition of α-smooth muscle actin, tissue inhibitors of metalloproteinases-1, and collagen-1 in rat model liver fibrosis. Open Access Macedonian Journal of Medical Sciences. 2020 Mar 3;8(A):287-92.

56. Tchounwou PB, Dasari S, Noubissi FK, Ray P, Kumar S. Advances in our understanding of the molecular mechanisms of action of cisplatin in cancer therapy. Journal of experimental pharmacology. 2021;13: 303.

57. Terzi S, Özgür A, Mercantepe T, Çeliker M, Tümkaya L, Dursun E. The effects of astaxanthin on salivary gland damage caused by cisplatin in the rat. Int J Res Med Sci. 2017 Apr;5(4):1410-4.

58. Valacchi G, Zanardi I, Lim Y, Belmonte G, Miracco C, Sticozzi C, Bocci V, Travagli V. Ozonated oils as functional dermatological matrices: Effects on the wound healing process using SKH1 mice. International Journal of Pharmaceutics. 2013 Dec 15;458(1):65-73.

59. Vongsak B, Sithisarn P, Gritsanapan W. Simultaneous HPLC quantitative analysis of active compounds in leaves of Moringa oleifera Lam. Journal of chromatographic science. 2014 Aug 1;52(7):641-5.

60. Zahawi SM. Impact of chamomile on the submandibular salivary gland of 5-Fluorouracil treated rabbits (histological and immunohistochemical study). J Clin Cell Immunol. 2015;6(366):2.

61. Zhang R, Yu Y, Deng J, Zhang C, Zhang J, Cheng Y, Luo X, Han B, Yang H. Sesamin ameliorates high-fat diet–induced dyslipidemia and kidney injury by reducing oxidative stress. Nutrients. 2016a May 9;8(5):276.

62. Zhang R, Yu Y, Hu S, Zhang J, Yang H, Han B, et al. Sesamin ameliorates hepatic steatosis and 579 inflammations in rats on a high-fat diet via LXRalpha and PPARalpha. Nutr Res. 2016b; 580 (36): 1022-1030.